ACS APPLIED MATERIALS & INTERFACES

Research Article

www.acsami.org

Protein Binding-Induced Surfactant Aggregation Variation: A New Strategy of Developing Fluorescent Aqueous Sensor for Proteins

Wenting Hu, Liping Ding,* Jianhua Cao, Lili Liu, Yuting Wei, and Yu Fang

Key Laboratory of Applied Surface and Colloid Chemistry of Ministry of Education, School of Chemistry and Chemical Engineering, Shaanxi Normal University, Xi'an 710062, P. R. China

Supporting Information

ABSTRACT: Novel strategies of developing fluorescent sensors for proteins are highly demanded. In this work, we particularly synthesized a cholesterol-derivatized pyrene probe. Its fluorescence emission is effectively tuned by the aggregation state of a cationic surfactant dodecyltrimethylammonium bromide (DTAB). The used probe/DTAB assemblies exhibit highly sensitive ratiometric responses to pepsin and ovalbumin egg (o-egg) with detection limits of 4.8 and 18.9 nM, respectively. The fluorescence changes indicate the protein−surfactant interaction leads to further aggregation of DTAB assemblies. The results from Tyndall effect and dynamic light scattering verify this assumption. The responses to pepsin and o-egg are due to their strong electrostatic or hydrophobic interaction with DTAB assemblies at pH 7.4. The present noncovalent supramolecular sensor represents a novel and simple strategy for sensing proteins, which is based on the encapsulated fluorophore probing the aggregation variation of the surfactant assemblies.

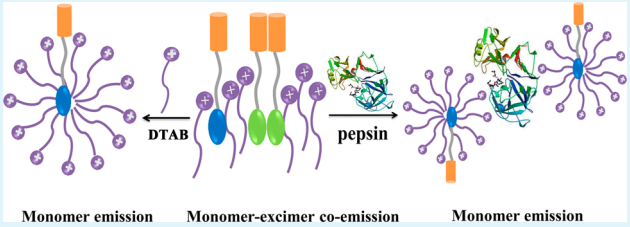

KEYWORDS: *supramolecular assembly, DTAB, pyrene, ratiometric sensor, pepsin*

INTRODUCTION

Proteins are one of the most important components in creatures and play fundamental but important roles in all kinds of biology processes. They are closely related to nutrition, enzyme, virus, immunity, material transportation, etc. Therefore, quantitative analysis and special recognition of protein is important for applications in proteomics, medical diagnostics, and pathogen detection.[1,2] Among various detection methods, fluorescent sensors have exhibited advantages in terms of sensitivity and selectivity. Therefore, developing fluorescent sensors for various proteins has gained increasing attention.

A variety of materials have been used to fabricate fluorescent sensors for proteins. For example, water-soluble conjugated polymers,[3,4] protein-printed polymers,[5] quantum dots[6,7] or carbon dots,[8] nanoparticles,[9,10] and graphene oxide[11] have been used to prepare fluorescent sensors for proteins. Usually, the materials used determine the detection environments, fluorescence stability or intensity, and biocompatibility of the sensor;[1] however, the strategy employed has more influence on the sensing behaviors of the sensor, such as sensitivity, selectivity, simplicity, etc. Many reported strategies used complex sensing processes or laborious synthesis. An appropriate but simple and powerful technique to tune the sensing properties is more attractive.[12]

To this end, researchers turn their interests to using supramolecular aggregation or assemblies to construct fluorescent sensors for proteins.[13] Surfactants, amphiphilic dendrimers, or polymers can self-assemble into various supramolecular architectures such as micelles and vesicles in aqueous solutions and then provide hydrophobic interiors for encapsulating fluorophores noncovalently.[14,15] Thus, the interaction of protein with supramolecular assemblies may induce changes of the assemblies and as a result vary the fluorescence emission properties of the encapsulated guest fluorophore. The noncovalent interaction between the fluorophore and the supramolecular aggregations can simplify the synthesis process.

Thayumanavan and co-workers have used micellar assemblies based on amphiphilic polymers,[16] polyelectrolyte and surfactant mixtures,[17,18] and amphiphilic dendrimers[19] to encapsulate small fluorophores to function as supramolecular sensors or arrays to proteins. One way to realize the sensing of proteins is based on the energy or electron transfer from the noncovalently encapsulated probe to the micelle-binding proteins.[16] Another way is dependent on the disassembly of dendrimer or polymer-based micellar containers upon binding proteins, and the concurrent release of guest fluorophores leads to fluorescence changes due to the variation of surrounding environments.[17−19] A similar strategy was used by Ji et al. They recently reported using supramolecular assemblies based on cationic surfactant and bioactive polyanion heparin to encapsulate pyrene to function as a selective sensor to heparin-binding proteins such as Tat peptide.[20] The binding of these proteins results in

Received: December 1, 2014
Accepted: February 9, 2015
Published: February 9, 2015

DOI: 10.1021/am508421n
ACS Appl. Mater. Interfaces 2015, 7, 4728−4736

disassembly of the heparin-CTAB assemblies and release of pyrene, which induces fluorescence changes.

Although supramolecular assemblies based on amphiphilic dendrimers or polymers exhibit interesting sensing behaviors to proteins, the synthesis of these amphiphilic dendrimers or polymers still needs some intensive synthesis efforts. Alternatively, small surfactant molecules are commercially available, and the use of surfactant assemblies will greatly simplify the process of preparing sensors for proteins. It is known that there are different types of interactions between proteins and surfactant molecules, which can give rise to protein−surfactant complexes that have different conformation from the pure surfactants.[21,22] Therefore, the conformation change of surfactant assemblies may be used to induce fluorescence variation of the encapsulated fluorophores.

Herein, we developed a fluorescent supramolecular sensor to detect proteins based on surfactant assemblies encapsulating a specially designed but simple fluorophore. Pyrene was selected as the signaling unit and was derivatized with cholesterol unit via a flexible diamine spacer. The presence of cholesterol unit leads to strong aggregation among pyrene units. The addition of cationic surfactant assemblies could affect the aggregation state of the probe molecules and vary its fluorescence emission. The interaction of proteins with selected surfactant assemblies leads to ratiometric responses of the encapsulated pyrene derivative. The present supramolecular sensor system exhibits highly sensitive and selective responses to pepsin and ovalbumin egg with detection limits as low as 4.8 and 18.9 nM, respectively.

EXPERIMENTAL SECTION

Chemicals and Instruments. 2,2-(Ethylenedioxy)bis(ethylamine) (EOA, 98%), cholesteryl chloroformate (98%), sodium dodecyl sulfate (SDS, ≥99%), Triton X-100 (TX100, ≥99%), decyltrimethylammonium bromide (DTAB, ≥98%), hexadecyltrimethylammonium bromide (CTAB, ≥99%), and 2X *N*-(2-hydroxyethyl)piperazine-*N*′-ethanesulfonic acid (HEPES) buffer solution (42 mM, pH 7.4) were all purchased from Sigma-Aldrich and used without further purification. HEPES buffer solution (10 mM, pH 7.4) was prepared by diluting the stock 2X HEPES buffer solution with water. SDS, TX100, DTAB, and CTAB were dissolved in neat water or HEPES buffer (10 mM, pH 7.4) to prepare aqueous solutions with required concentrations. All proteins including bovine serum albumin (≥98%), lysozyme (from chicken egg, lyophilized powder, ≥90%), trypsin (from bovine pancreas, 10,000 BAEE units/mg protein), pepsin (from porcine gastric mucosa, lyophilized powder, ≥2500 units/mg protein), *β*-lactoglobulin (from bovine milk, ≥90%), cytochrome c (from bovine heart, ≥95%), and ovalbumin egg (from chicken egg white, lyophilized powder, ≥98%) were purchased from Chemical Company of China (Shanghai) and used as supplied. Their stock solutions (2.5×10^{-4} mol/L) were prepared by dissolving proteins in 10 mM HEPES buffer (pH 7.4) and stored at 0−4 °C. All aqueous solutions were prepared from Milli-Q water (18.2 MΩ cm at 25 °C).

Melting point was measured on ×5 microscopic melting point meter (Beijing Tech. Instrument). The ^{1}H NMR spectra of the synthesized chemicals were obtained on a Bruker Avance 400 MHz NMR spectrometer. The high-resolution mass spectra (MS) were acquired in electrospray ionization (ESI) positive mode using a Bruker Maxis UHR-TOF Mass Spectrometer. Steady-state fluorescence spectra were measured on a time-correlated single photon-counting fluorescence spectrometer (FLS920, Edinburgh Instruments) with xenon light as excitation source, and all samples were excited at 353 nm. The particle size distribution was measured on a Malvern Zetasizer Nano-ZS90.

Synthesis of Cholesterol-Modified Pyrene Probe (Py-EOA-Chol). The synthesis process of the cholesterol derivative of pyrene-based fluorophore is depicted in Scheme 1. The starting material, pyrenesulfonyl chloride (PSC), was synthesized by adopting a literature method.[23] The first step reaction to synthesize Py-EOA was described in detail in our previously reported work.[24] The second step reaction is as follows: to the solution of Py-EOA (0.226 g, 0.548 mmol) in CH_2Cl_2 (5 mL) containing catalytic amount of triethylamine, cholesterol chloroformate (0.369 g, 0.822 mmol) in CH_2Cl_2 (5 mL) was added. The reaction mixture was stirred overnight at room temperature under nitrogen atmosphere. The organic solution was evaporated in vacuo. The resulting solid was purified by column chromatography on silica gel with petroleum ether/ethyl acetate (1.5:1, v/v) as the eluent. The purified Py-EOA-Chol was collected as pale yellow solid with a yield of 33.3% (~0.15 g): mp 72.2−73.7 °C. ^{1}H NMR (400 MHz, $CDCl_3$, ppm): δ 9.00 (d, J = 9.2 Hz, 1H), 8.71 (d, J = 8.2 Hz, 1H), 8.21 (m, 7H), 5.64 (s, 1H), 5.29 (s, 1H), 5.12 (s, 1H), 4.46 (s, 1H), 3.32 (ddd, J = 74.8, 38.6, 4.7 Hz, 12H), and 1.97−0.66 (43H). FTIR (KBr plate, cm^{-1}): 3341 (−NH), 3060 (Ar−H), 2937 ($-CH_2$), 1700 (−C═O), 1589 (Ar C═C), 1159 (O═S═O), 1100 (−C−O−C). MS (ESI, m/z): $[M + H]^+$ calcd. for $C_{50}H_{68}N_2O_6S$, 847.4696; found, 847.4699.

Scheme 1. Synthesis of Cholesterol-Derivatized Pyrene Probe Py-EOA-Chol

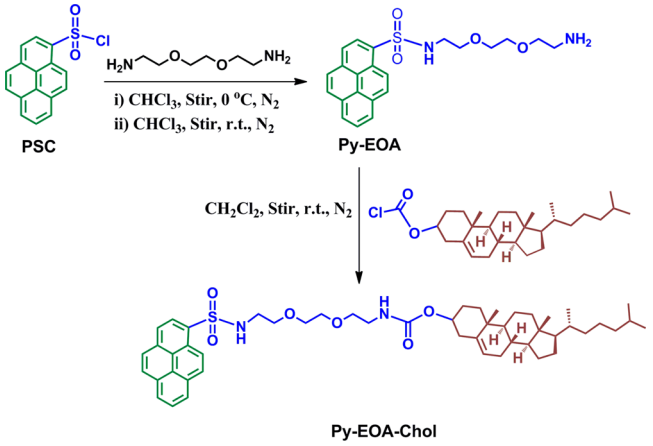

RESULTS AND DISCUSSION

Fluorescence Emission of Py-EOA-Chol in Neat Solvents and Micellar Solutions. We first examined the fluorescence emission of Py-EOA-Chol (0.5 μM) in neat solvents, namely, the good solvent acetonitrile and the poor solvent water. As shown in Figure 1a, Py-EOA-Chol exhibits quite different emission in the two solvents. In acetonitrile, the fluorophore displays only monomer emission at 379 and 399 nm, suggesting it is unimolecularly dispersed in the good solvent. On the contrary, in water, Py-EOA-Chol shows dominant excimer emission centered at 498 nm accompanied by very weak monomer emission, indicating the hydrophobic pyrene moieties tend to aggressively aggregate in the poor solvent, which leads to unstable fluorescence emission in water. Over a period of 45 min, the fluorescence emission appears very stable in acetonitrile, but continuously decreases in water (Figure S1, Supporting Information).

We then measured the fluorescence emission of Py-EOA-Chol in different micellar solutions to examine surfactant effect. Three surfactants carrying different surface charges were used, which include SDS (the anionic one), DTAB (the cationic one), and TX100 (the neutral one). The concentrations of SDS (12 mM), DTAB (16 mM), and TX100 (0.5 mM) were controlled above their corresponding critical micelle concen-

DOI: 10.1021/am508421n
ACS Appl. Mater. Interfaces 2015, 7, 4728−4736

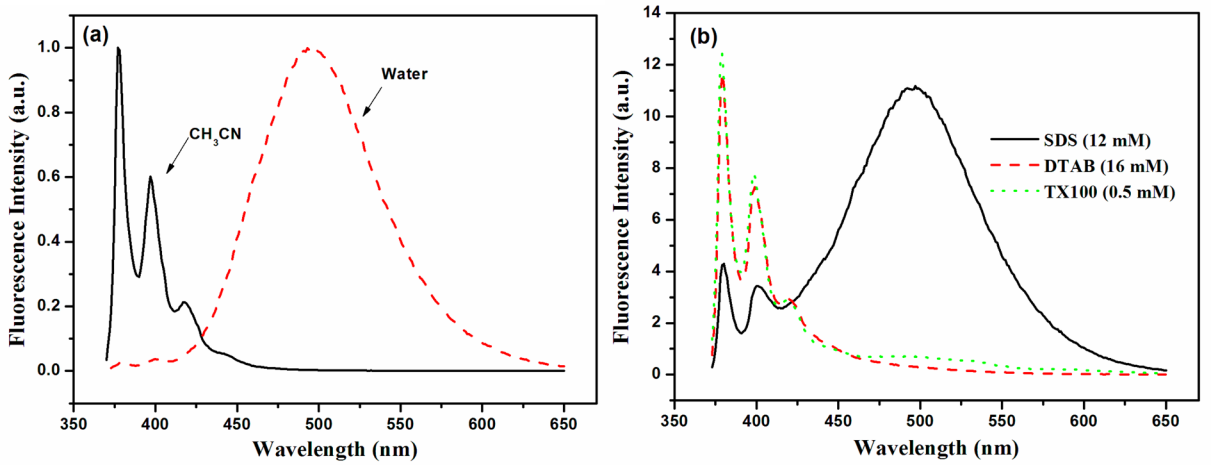

Figure 1. Fluorescence emission spectra of Py-EOA-Chol (0.5 μM) in neat solvents (a) and in different micellar solutions (b) (λ_{ex} = 353 nm).

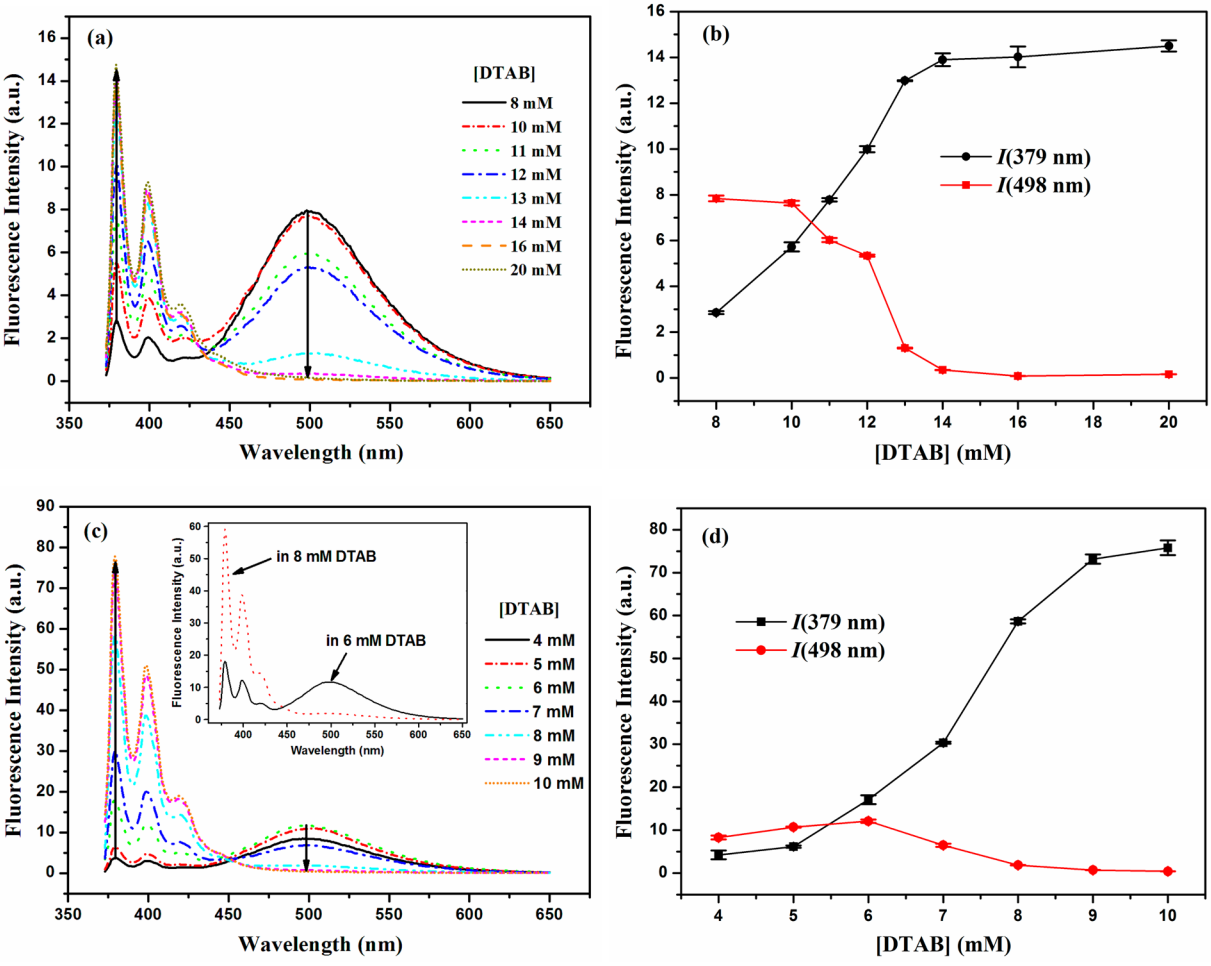

Figure 2. (a) Fluorescence emission spectra of Py-EOA-Chol (0.5 μM) in a series of aqueous solutions with different DTAB concentrations; (b) fluorescence intensity of monomer emission at 379 nm and excimer emission at 498 nm of Py-EOA-Chol (0.5 μM) in aqueous solutions as a function of DTAB concentration; (c) fluorescence emission spectra of Py-EOA-Chol (0.5 μM) in a series of HEPES buffer solutions (10 mM, pH 7.4) with different DTAB concentrations. (inset) Enlarged fluorescence emission of Py-EOA-Chol (0.5 μM) in 6 mM and 8 mM DTAB HEPES buffer solutions; and (d) fluorescence intensity of monomer emission at 379 nm and excimer emission at 498 nm of Py-EOA-Chol (0.5 μM) in HEPES buffer solutions (10 mM, pH 7.4) as a function of DTAB concentration (λ_{ex} = 353 nm). The error bars represent the standard deviation of three measurements.

tration (CMC) at 8, 14, and 0.24 mM, respectively,[25] so as to provide micellar solutions. The resulting emission spectra are shown in Figure 1b. In SDS micelles, the fluorophore exhibits both the structured monomer emission and the broad excimer emission. The dominative excimer emission indicates strong aggregation still occurs in SDS micellar solutions and that the

DOI: 10.1021/am508421n
ACS Appl. Mater. Interfaces 2015, 7, 4728−4736

fluorophore is not monomolecularly incorporated in SDS micelles. Differently, the presence of DTAB or TX100 micelles leads to loss of the excimer emission and gives rise to significant monomer emission. These results suggest that the fluorophore is monomolecularly encapsulated in the cationic and neutral micelles, which breaks its aggregation in water. Moreover, the fluorescence stability of the fluorophore in water is remarkably improved in the presence of surfactant micelles (Figure S2, Supporting Information).

DTAB Concentration Effect on the Fluorescence Emission of Py-EOA-Chol. Considering DTAB micelles possessing positive charges and having potential of interacting differently with different proteins, we chose Py-EOA-Chol/DTAB system for further photophysical and sensing studies. We first systematically investigated DTAB concentration (C_{DTAB}) effect on the fluorescence emission of Py-EOA-Chol to evaluate the modulation behavior of surfactant assemblies. To do so, a series of aqueous solutions containing different concentrations of DTAB were prepared and used to dissolve the same amount of fluorescent probe (0.5 μM). The fluorescence emission spectra of these aqueous solutions were measured separately under the same test conditions. The results are displayed in Figure 2a,b. It can be seen that the surfactant concentration has a distinct effect both on the profile and the intensity of the fluorescence emission of Py-EOA-Chol. In the solution with the lowest C_{DTAB} at 8 mM, the probe shows dominant excimer emission accompanied by weaker monomer emission, suggesting the fluorophore still exists as strong aggregates. The increasing C_{DTAB} leads to remarkable enhancement of the monomer emission along with continuously decreasing excimer emission (Figure 2b). Over the range from 9 to 13 mM DTAB, the probe exhibits monomer−excimer coemission (Figure 2a). Such results indicate that the aggregation of the fluorophore is gradually disrupted by the increasingly aggregated DTAB assemblies. When C_{DTAB} reaches 14 mM (the CMC of DTAB), the excimer emission totally vanishes, and the probe illustrates total monomer emission, suggesting that the fluorophore is monomolecularly distributed in DTAB micelles. Further increasing C_{DTAB} beyond 14 mM has low influence on the emission. Such results indicate that the variation of DTAB assembly state (e.g., from premicelle to micelle) could significantly influence the aggregation states of the encapsulated fluorophore and its fluorescence emission. The tuning of fluorescence emission of the cholesterol-derivatized pyrene probe by different DTAB aggregates is schematically illustrated in Scheme 2.

For measuring the sensing behavior to proteins, a buffer solution with physiological pH is needed. Therefore, the DTAB concentration effect on the fluorescence emission of Py-EOA-Chol was also examined in HEPES buffer solution (10 mM, pH 7.4). Similarly, a series of HEPES buffer solutions containing different concentration of DTAB with the same amount of the fluorescent probe (0.5 μM) were used for the fluorescence emission measurements. The results are displayed in Figure 2c,d. Clearly, the change of DTAB concentration could also significantly vary the fluorescence emission of the probe in the buffer solution. Along increasing DTAB concentration, the fluorescence emission also changes from excimer-dominant emission (4−5 mM DTAB) to monomer−excimer coemission (6−7 mM DTAB) to monomer-dominant emission (≥8 mM) (Figure 2c), where the monomer intensity continuously increases along with decreased excimer emission (Figure 2d). According to what was observed in water, the above results

Scheme 2. DTAB Assemblies Interacting with Py-EOA-Chol and Influencing the Fluorescence Emission of the Pyrene Derivative

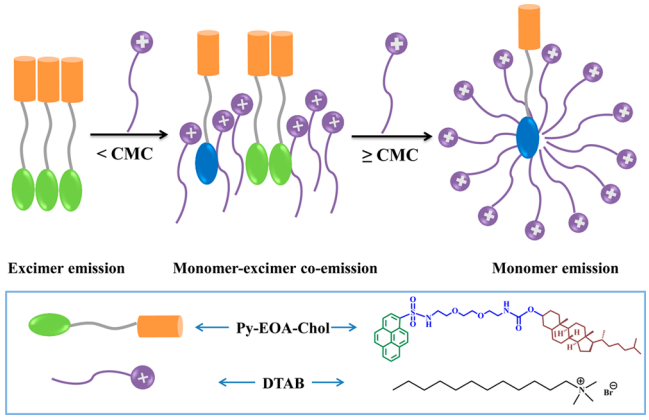

suggest that DTAB micelles form at 8 mM in HEPES solution. The reduction of CMC for DTAB may be due to the complex composition of the buffer solution that alters the assembling behavior of DTAB. The abrupt change of fluorescence emission occurs from 6 to 8 mM DTAB (c.f. the inset of Figure 2c), indicating the probe is also very sensitive to the aggregation changes of DTAB assemblies from premicelle to micelle in the HEPES buffer solution and reports the DTAB aggregation changes from its fluorescence variation. Considering that the potential protein−DTAB interaction may also induce aggregation variation of DTAB assemblies, we next examined the sensing behavior of Py-EOA-Chol/DTAB platform to proteins.

Py-EOA-Chol/DTAB Platform Sensing Pepsin in HEPES Solution. Since the abrupt change of fluorescence emission occurs over the range of 6−8 mM DTAB in HEPES solution, we controlled C_{DTAB} of Py-EOA-Chol/DTAB platform at both 6 and 8 mM to check which can sense the assembly variation and further detect protein. Pepsin was selected as the target protein since its isoelectric point (pI) is 1.0 and should possess negative charges at pH 7.4. Therefore, it may induce significant variation of DTAB aggregates due to the potential electrostatic interaction. It turned out that the one with 8 mM DTAB does not vary upon addition of pepsin (Figure S3, Supporting Information), and the one with 6 mM DTAB indeed responds to the presence of pepsin. Therefore, C_{DTAB} of the fluorophore/surfactant assemblies was controlled at 6 mM and used for the following sensing studies.

Figure 3 illustrates the fluorescence variation of the sensor platform upon addition of pepsin at 0.06 and 0.6 μM. Clearly, the addition of pepsin induces monomer enhancement and excimer reduction via an isoemissive point at 443 nm, rendering the present supramolecular system a ratiometric sensor for pepsin. This fluorescence variation is similar to that induced by increasing DTAB concentration, indicating that the addition of pepsin leads to further assembling of DTAB molecules. This may explain why the sensor platform with 8 mM DTAB does not respond to protein binding. The fluorescence variation of the probe exhibits both concentration-dependent and time-dependent behaviors. As shown in Figure 3a, over a period of 30 min, the sensor system still shows 50% remaining excimer emission in the presence of 0.06 μM pepsin. By comparison, 10-fold concentrated pepsin (0.6 μM) leads to more significant excimer reduction and monomer enhancement (Figure 3b). Moreover, the change from monomer−excimer coemission

DOI: 10.1021/am508421n
ACS Appl. Mater. Interfaces 2015, 7, 4728−4736

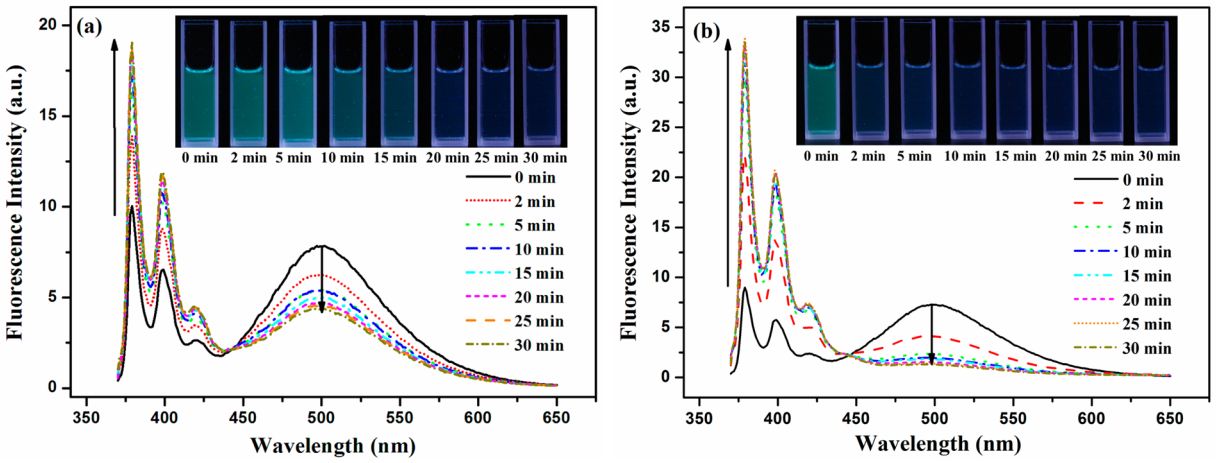

Figure 3. Fluorescence spectra of Py-EOA-Chol/DTAB (0.5 μM/6 mM) in HEPES buffer solution (10 mM, pH 7.4) upon addition of (a) 0.06 μM and (b) 0.6 μM of pepsin over a period of 30 min (λ_{ex} = 353 nm). (insets) Photos of the sensor solution upon addition of pepsin for different periods of time under the illumination of 365 nm UV light.

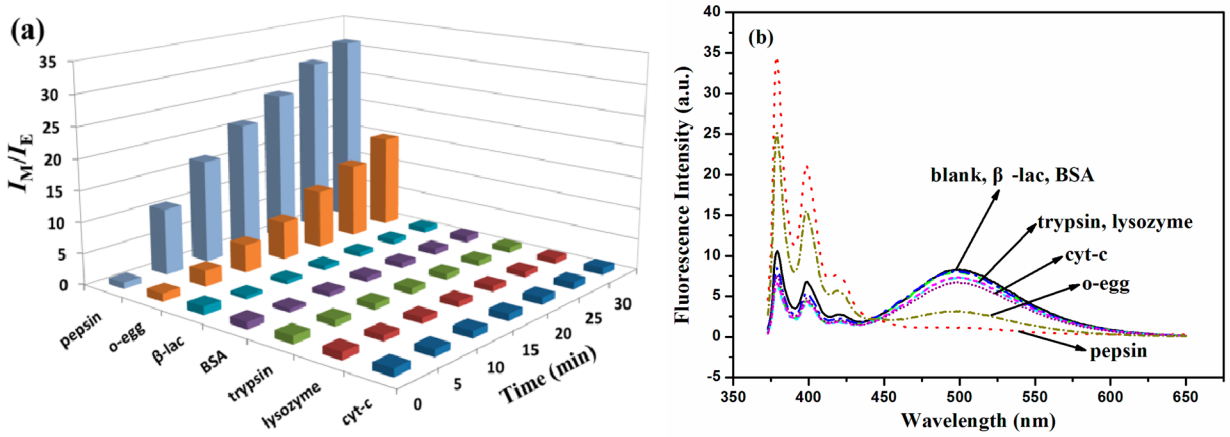

Figure 4. (a) The ratio of monomer to excimer intensity I_M/I_E of the Py-EOA-Chol/DTAB (0.5 μM/6 mM) system in the presence of various proteins (1.0 μM) as a function of incubation time. (b) Fluorescence emission spectra of Py-EOA-Chol/DTAB system after incubation with a series of proteins (1.0 μM) for 10 min (λ_{ex} = 353 nm).

state to the final monomer-dominant emission is faster in the presence of higher concentration of pepsin, where only 10 min is needed to reach a nearly balanced state for addition of 0.6 μM pepsin. This is also evidenced by the emission color change of the sensor solution upon the incubation time of pepsin (insets of Figure 3). In the presence of 0.06 μM pepsin, the green emission is gradually faded and varies to blue emission over a period of 30 min, whereas, in the presence of 0.6 μM pepsin, the process takes less than 10 min.

Py-EOA-Chol/DTAB Platform Sensing Different Proteins in HEPES Solution. We then measured the fluorescence responses of the sensor system to a series of proteins (1.0 μM) with different pI values. The tested proteins include pepsin (pI = 1.0), ovalbumin egg (o-egg, pI = 4.7), bovine serum albumin (BSA, pI = 4.7), β-lactoglobulin (β-lac, pI = 5.1−5.3), trypsin (pI = 10.5), cytochrome c (cyt-c, pI = 10.7), and lysozyme (pI = 11.0−11.35). It turns out that besides pepsin, only o-egg can induce remarkable fluorescence variation. As illustrated in Figure 4a, the intensity ratio of monomer to excimer I_M/I_E gradually increases only in the presence of pepsin and o-egg over a period of 30 min of incubation. However, all the other proteins induce slight fluorescence variation. Figure 4b illustrates the fluorescence emission spectra of the fluorophore/DTAB platform that were recorded after incubation with various proteins for 10 min. Both pepsin and o-egg lead to monomer enhancement and excimer reduction. It is just that the variation of both monomer and excimer is larger for pepsin than for o-egg. The fluorescence spectra slightly change upon the addition of the other five proteins. This result suggests that the present fluorophore/surfactant assemblies could probably function as a sensor for both pepsin and o-egg.

Sensitivity of Py-EOA-Chol/DTAB to Pepsin and Ovalbumin Egg. The fluorescence responses of the sensor system to pepsin and o-egg at various concentrations were further measured. For these measurements, the fluorescence spectra of the testing solution in the presence of each concentration of pepsin or o-egg were separately recorded after 10 min of incubation and illustrated in one map. The results are shown in Figure 5. The sensor system exhibits a ratiometric response to both proteins, where the enhanced monomer emission is accompanied by decreased excimer emission along increasing protein concentration. The fluorescence ratio of monomer to excimer I_M/I_E exhibits a linear relationship to the concentration of the two proteins as revealed by the insets. In the case of sensing pepsin, it turns out there are two linear detection windows; one is over the range

DOI: 10.1021/am508421n
ACS Appl. Mater. Interfaces 2015, 7, 4728−4736

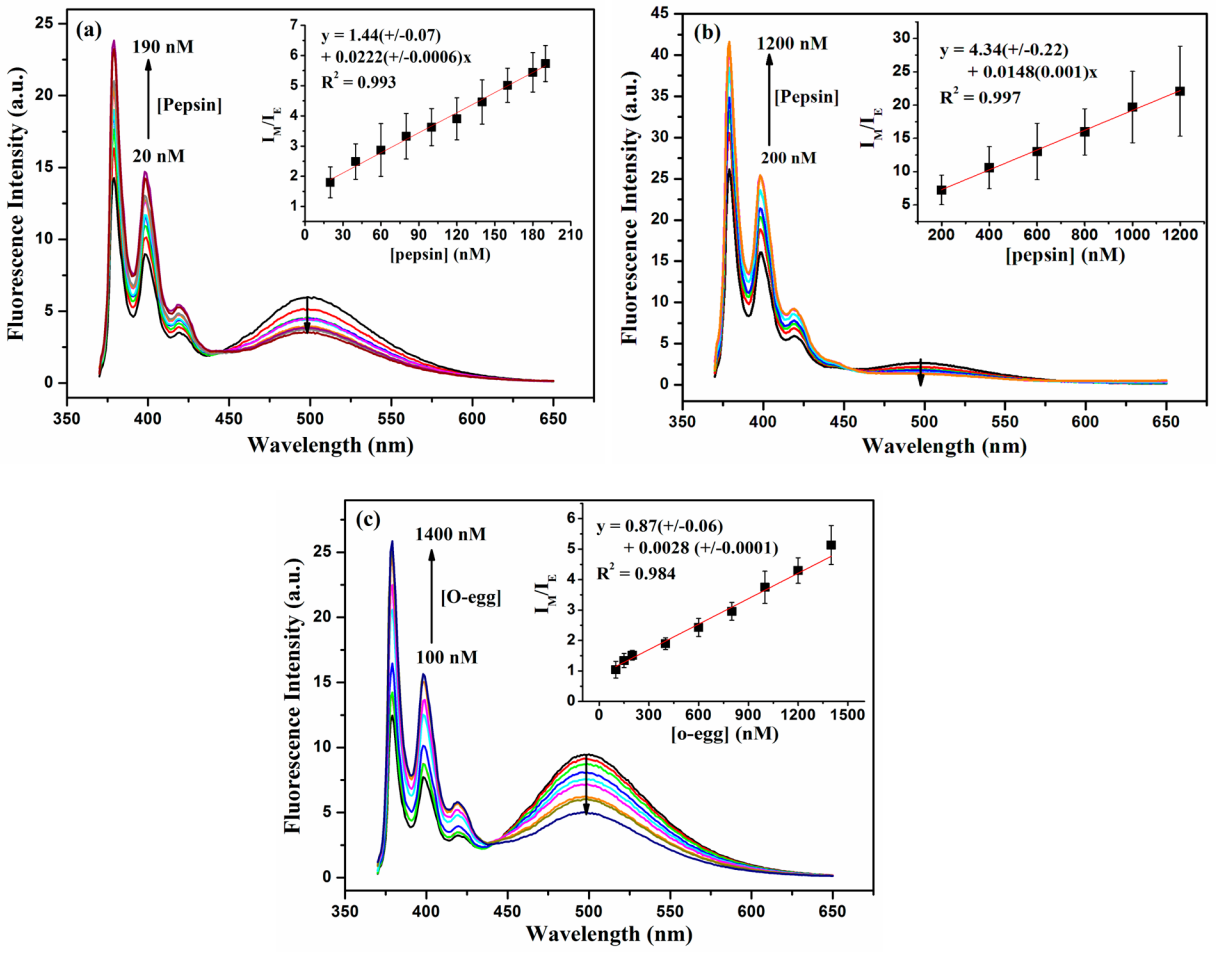

Figure 5. Fluorescence emission of Py-EOA-Chol/DTAB (0.5 μM/6 mM) upon titration of pepsin (a, b) and o-egg (c) in 10 mM HEPES buffer solution (pH = 7.40) (λ_{ex} = 353 nm). (insets) Fluorescence intensity ratio of monomer to excimer I_M/I_E as a function of protein concentration. The error bars represent the standard deviation of three measurements.

from 20 to 190 nM (Figure 5a), and the other is over the range from 200 to 1200 nM (Figure 5b). For the sensing of o-egg, the working concentration window is 100 to 1400 nM. The detection limits (DLs) of the present sensor system to pepsin and o-egg are determined to be 4.8 nM (0.168 μg mL^{-1}) and 18.9 nM (0.837 μg mL^{-1}), respectively, according to the 3σ IUPAC criteria. Presently, there are several methods that have been reported to detect these two proteins, such as chromatographic methods,[26−28] imprinting hybrid thin films or imprinting polymers,[29,30] fluorescent nanoparticles,[9] and voltammetric immunosensor.[31] By comparison, chromatographic analysis exhibits lower sensitivity at milligram levels,[26−28] while sensitivity information is not available for imprinting methods.[29,30] The fluorescent nanoparticles show competitive sensitivity to pepsin (DL of 0.256 μg mL^{-1}); however, this method needs much longer incubation time (180 min) for protein detection.[9] Voltammetric immunosensor presents higher sensitivity toward o-egg (DL of 0.83 pg mL^{-1})[31] but not to pepsin. Therefore, the present supramolecular fluorescent sensing platform represents a fast and highly sensitive fluorescent sensor to these two proteins. Moreover, the present method is simple by just mixing fluorophore and surfactant assemblies and is easy to operate for detection process.

Sensing Mechanism Studies. It is necessary to understand the sensing mechanism of the present supramolecular sensors. As mentioned earlier, the ratiometric fluorescence changes induced by the added pepsin or o-egg is similar to those fluorescence variations produced by increasing surfactant concentration. This suggests that the added protein probably leads to further assembling of DTAB molecules from less-aggregated state to micelle-like conformation, which accounts for the ratiometric fluorescence changes of the probe.

To deeply understand the role of DTAB assemblies in the sensing process to pepsin and o-egg, we further measured the fluorescence responses of the probe to these two proteins in the absence of DTAB and in the presence of lower concentration of DTAB assemblies. It turned out that these two proteins neither produced ratiometric fluorescence responses in the absence of DTAB assemblies (Figure S4, Supporting Information)[32] nor in the presence of very low concentration of DTAB (e.g., 2 mM, Figure S5, Supporting Information). In the solution containing 4 mM DTAB, the added proteins induced similar ratiometric responses of the probe (Figure S6, Supporting Information), but the extent is much smaller compared to the responses in 6 mM DTAB solution. These results indicate that, on one hand, the protein itself does not produce ratiometric variation of the probe and the DTAB assemblies play an important role in realizing ratiometric responses to proteins; on the other hand, the sensing process is highly dependent on the surfactant concentration, namely, the aggregation state of DTAB assemblies. Moreover, the extent of protein-induced fluores-

DOI: 10.1021/am508421n
ACS Appl. Mater. Interfaces 2015, 7, 4728−4736

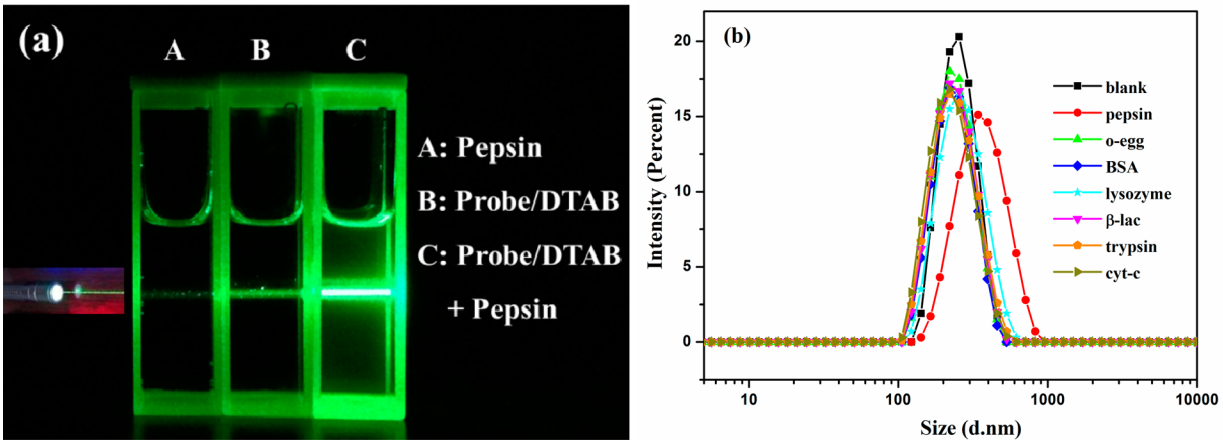

Figure 6. (a) Tyndall scattering of Py-EOA-Chol/DTAB (0.5 μM/6 mM) upon addition of 0.6 μM pepsin. (b) Size distribution of Py-EOA-Chol/DTAB (0.5 μM/6 mM) before and after addition of various proteins (0.6 μM).

cence variation in different concentration of DTAB assemblies shows positive correlation with the extent of fluorescence variation induced by increasing DTAB concentration. Therefore, the protein-induced fluorescence variation should be due to the changes of the aggregation state of DTAB assemblies, which could be induced by protein−surfactant interaction.

We also examined the fluorescence responses of the probe to these two proteins in a similar surfactant assembly, namely, CTAB, which possesses the same cationic headgroup but with a longer fat chain length. Similarly, the changes of CTAB assemblies can induce fluorescence variation of the probe, where increasing CTAB concentration leads to the fluorescence emission changes from excimer-dominated emission to monomer−excimer coemission to monomer-dominated emission (Figure S7, Supporting Information). The abrupt fluorescence change occurs over a CTAB concentration range from 0.08 to 0.15 mM. We then measured the fluorescence responses of the probe in 0.08 mM CTAB to both pepsin and o-egg. Similar ratiometric responses to these two proteins were observed for the CTAB system (Figure S8, Supporting Information), although the sensitivity is smaller than the DTAB system. However, when the same experiments were conducted in the 0.15 mM CTAB solution, no ratiometric responses were observed. Only slight fluorescence quenching occurred upon addition of 0.6 μM of pepsin or o-egg (Figure S9, Supporting Information). These results once again approve the correlation between the protein-induced fluorescence variation and the surfactant assembly change-induced fluorescence variation, suggesting the protein-induced aggregation changes of surfactant assemblies are responsible for fluorescence variation of the probe.

To confirm the above assumption, we checked the Tyndall effect of the supramolecular sensor upon addition of pepsin. As seen in Figure 6, the solution of pepsin protein alone shows a very weak Tyndall scattering. The surfactant solution containing the probe exhibits stronger Tyndall scattering, which may be due to the presence of premicelles of DTAB assemblies at 6 mM in the HEPES buffer solution. After adding pepsin (0.6 μM), the surfactant solution displays a stunning Tyndall scattering, proving a strong aggregation indeed forms that could be micelles of DTAB. The increased Tyndall effect induced by protein is also observed for o-egg and β-lac, but with much smaller extent (Figure S10a,c, Supporting Information). However, the addition of other examined proteins produces unnoticeable changes (Figure S10b,d−f), Supporting Information). Such results reveal that the extent of protein-induced aggregation variation of DTAB assemblies is highly correlated to the sensing responses to these proteins.

We also used dynamic light scattering (DLS) to measure the size changes of the supramolecular sensor platform after addition of various proteins. The results of DLS measurements are displayed in Figure 6b. The diameter of the sensor assembly prior to the addition of proteins was ca. 234 nm. Upon addition of proteins (0.6 μM), the only apparent change of the diameter of the assembly is observed for pepsin. The addition of pepsin leads to a great diameter enhancement to ca. 320 nm, indicating larger aggregation forms. However, the addition of all the other proteins produces slight size variation of the sensor assembly, suggesting smaller aggregation variation induced by these proteins.

The highest extent of surfactant aggregation variation induced by pepsin may be because it has the lowest pI value (1.0). This pI value renders pepsin possessing more negative charges at pH 7.4 and a resulting stronger electrostatic interaction with DTAB assemblies. The pI values goes up in the order of o-egg (pI 4.7), BSA (pI 4.7), β-lac (pI 5.1−5.3), trypsin (pI 10.5), cyt-c (pI = 10.7), and lysozyme (11.0), which make them possess less negative charges or even positive charges at neutral pH. Thus, these proteins have weaker electrostatic attraction or even electrostatic repulsion with DTAB assemblies and then produce less extent of aggregation variation of surfactant assemblies, which explains the weaker sensitivity to o-egg and negative responses to other proteins. An exception is BSA, which has the same pI value with o-egg but produces slight fluorescence changes. This difference may be due to their different structure. It is known that there are also hydrophobic interactions between surfactants and proteins.[22] The surface of o-egg is significantly more hydrophobic than the surface of BSA,[53] which may render o-egg a stronger hydrophobic interaction with DTAB assemblies and induce more apparent aggregation variation.

We also evaluated the role of cholesterol unit of the probe in the sensing process. First, we particularly synthesized a control compound (Py-EOA-AC) that uses a methyl group to replace the cholesterol group (Scheme S1, Supporting Information). Then we examined the sensing behavior of this compound under the same experimental conditions. Interestingly, this control supramolecular system, Py-EOA-AC/DTAB, displays

DOI: 10.1021/am508421n
ACS Appl. Mater. Interfaces 2015, 7, 4728−4736

only monomer emission in HEPES buffer solutions (Figure S11, Supporting Information). The further addition of either pepsin (from 0.1 to 1.2 μM, Figure S12a, Supporting Information) or o-egg (from 0.1 to 1.4 μM, Figure S12b, Supporting Information) produces slight fluorescence variation. These results suggest that the cholesterol unit plays an important role in forming aggregates among probe molecules for excimer emission in 6 mM DTAB solution. Then, the aggregates among probe molecules can be tuned by the protein−surfactant interaction, and the resulting fluorescence changes can be used to report the presence of proteins. Namely, the cholesterol unit is a critical segment for the probe design and for realizing the noncovalent sensing of proteins.

Thus, a clear sensing process of the supramolecular sensor to proteins can be drawn now. First, the cholesterol-modified pyrene probe tends to form strong aggregates in aqueous solution and emit strong excimer emission. This strong aggregation was modulated by DTAB assemblies. The use of 6 mM DTAB assemblies realized interruption of the strong aggregates among probes, leading to monomer and excimer coemission. The added pepsin has a strong electrostatic interaction with DTAB assemblies and induces further aggregation of DTAB assemblies from premicelles to micelles, which totally breaks the aggregates among probes and realizes single probe encapsulation in DTAB assemblies. As a result, the monomer−excimer coemission changes to monomer-dominant emission upon the addition of pepsin (Scheme 3).

Scheme 3. Py-EOA-Chol/DTAB Supramolecular Sensor Noncovalent Responding to Pepsin

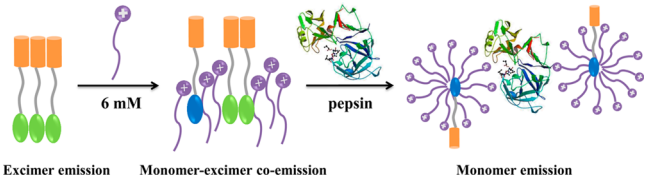

The present work provides a novel and simple strategy for developing fluorescent sensors for proteins in aqueous solutions, where protein binding induces surfactant aggregation variation and further leads to fluorescence changes of the encapsulated fluorophore. This strategy represents a noncovalent method different from the ones proposed by Thayumanavan[17,18] and Ji.[20] Their strategies are more based on protein-induced disassembling of supramolecular assemblies and result in fluorescence quenching of the encapsulated fluorophores. Compared to fluorescence quenching, ratiometric sensing of proteins provided by the present strategy is more reliable since it can minimize the background signals.[34]

CONCLUSION

In summary, we have developed a novel noncovalent supramolecular sensor for proteins based on a cationic surfactant assembly encapsulating a cholesterol-modified pyrene probe, Py-EOA-Chol. Surfactant concentration effect studies reveal that the fluorescence emission of Py-EOA-Chol can be tuned by the aggregation state of DTAB assemblies. The change from premicelle to micelle leads to the fluorescence variation of the probe from monomer−excimer coemission to monomer-dominant emission. The tuning ability by DTAB aggregates can be extended to sensing proteins in aqueous solution. The selected fluorophore/DTAB assemblies with fixed DTAB concentration exhibit sensitive ratiometric responses to pepsin and o-egg with detection limits of 4.8 and 18.9 nM, respectively. Tyndall effect studies and DLS measurements verify the aggregation changes of supramolecular assemblies induced by proteins.

The present work represents a novel and simple strategy for sensing proteins, which is based on the sensitivity of the encapsulated probe to the aggregation variation of the surfactant assemblies. This noncovalent method can be easily extended to using other fluorophores that can form aggregates and can be applied to sensing various targets that can vary the aggregation of supramolecular assemblies.

ASSOCIATED CONTENT

Supporting Information

The synthesis of control compound (Py-EOA-AC), fluorescence emission stability of Py-EOA-Chol in neat solvents and in micellar solutions, Tyndall scattering, fluorescence emission of control compound and sensing behaviors. This material is available free of charge via the Internet at http://pubs.acs.org.

AUTHOR INFORMATION

Corresponding Author

*Phone: +86-29-81530789. Fax: +86-29-81530727. E-mail: dinglp33@snnu.edu.cn.

Notes

The authors declare no competing financial interest.

ACKNOWLEDGMENTS

The authors acknowledge the financial supports from National Natural Science Foundation of China (21173142), Ministry of Education of China (NCET-12-0895), Shaanxi Provincial Department of Science and Technology (2011KJXX48), the Program of Introducing Talents of Discipline to Universities (B14041), Program for "Changjiang Scholars and Innovative Research Team in University" (IRT_14R33), and the Fundamental Research Funds for the Central Universities (GK201301006).

REFERENCES

(1) Wang, L.; Liu, Y.; Yang, J. X.; Tao, X. T.; Liu, Z. Microstructured Fluorescent Biosensor Based on Energy Migration for Selective Sensing of Metalloprotein. *Chem. Commun.* **2012**, *48*, 5742−5744.

(2) Tekin, H. C.; Gijs, M. A. M. Ultrasensitive Protein Detection: A Case for Microfluidic Magnetic Bead-Based Assays. *Lab Chip* **2013**, *13*, 4711−4739.

(3) Lee, K.; Povlich, L. K.; Kim, J. Recent Advances in Fluorescent and Colorimetric Conjugated Polymer-Based Biosensors. *Analyst* **2010**, *135*, 2179−2189.

(4) Fan, C.; Plaxco, K. W.; Heeger, A. J. High-Efficiency Fluorescence Quenching of Conjugated Polymers by Proteins. *J. Am. Chem. Soc.* **2002**, *124*, 5642−5643.

(5) Takeuchi, T.; Hishiya, T. Molecular Imprinting of Proteins Emerging as a Tool for Protein Recognition. *Org. Biomol. Chem.* **2008**, *6*, 2459−2467.

(6) Gao, X.; Liu, X.; Lin, Z.; Liu, S.; Su, X. $CuInS_2$ Quantum Dots as a Near-Infrared Fluorescent Probe for Detecting Thrombin in Human Serum. *Analyst* **2012**, *137*, 5620−5624.

(7) Liu, S.; Na, W.; Pang, S.; Shi, F.; Su, X. A Label-Free Fluorescence Detection Strategy for Lysozyme Assay Using $CuInS_2$ Quantum Dots. *Analyst* **2014**, *139*, 3048−3054.

(8) Maiti, S.; Das, K.; Das, P. K. Label-Free Fluorimetric Detection of Histone Using Quaternized Carbon Dot-DNA Nanobiohybrid. *Chem. Commun.* **2013**, *49*, 8851−8853.

DOI: 10.1021/am508421n
ACS Appl. Mater. Interfaces 2015, 7, 4728−4736

(9) Li, W.; Gao, Z.; Su, R.; Qi, W.; Wang, L.; He, Z. Scissor-Based Fluorescent Detection of Pepsin Using Lysozyme-Stabilized Au Nanoclusters. *Anal. Methods* **2014**, *6*, 6789−6795.
(10) Kim, B.-H.; Yoon, I. S.; Lee, J.-S. Masking Nanoparticle Surfaces for Sensitive and Selective Colorimetric Detection of Proteins. *Anal. Chem.* **2013**, *85*, 10542−10548.
(11) Li, S.; Mulloor, J. J.; Wang, L.; Ji, Y.; Mulloor, C. J.; Micic, M.; Orbulescu, J.; Leblanc, R. M. Strong and Selective Adsorption of Lysozyme on Graphene Oxide. *ACS Appl. Mater. Interfaces* **2014**, *6*, 5704−5712.
(12) Ghosh, A. K.; Bandyopadhyay, P. A Simple Strategy for Charge Selective Biopolymer Sensing. *Chem. Commun.* **2011**, *47*, 8937−8939.
(13) Seo, S.; Kim, J.; Jang, G.; Kim, D.; Lee, T. S. Aggregation-Deaggregation-Triggered, Tunable Fluorescence of an Assay Ensemble Composed of Anionic Conjugated Polymer and Polypeptides by Enzymatic Catalysis of Trypsin. *ACS Appl. Mater. Interfaces* **2014**, *6*, 918−924.
(14) Yesilyurt, V.; Ramireddy, R.; Thayumanavan, S. Photoregulated Release of Noncovalent Guests from Dendritic Amphiphilic Nanocontainers. *Angew. Chem., Int. Ed.* **2011**, *50*, 3038−3042.
(15) Rajasekhar Reddy, R.; Raghupathi, K. R.; Torres, D. A.; Thayumanavan, S. Stimuli Sensitive Amphiphilic Dendrimers. *New J. Chem.* **2012**, *36*, 340−349.
(16) Sandanaraj, B. S.; Demont, R.; Thayumanavan, S. Generating Patterns for Sensing Using a Single Receptor Scaffold. *J. Am. Chem. Soc.* **2007**, *129*, 3506−3507.
(17) Savariar, E. N.; Ghosh, S.; Gonzalez, D. C.; Thayumanavan, S. Disassembly of Noncovalent Amphiphilic Polymers with Proteins and Utility in Pattern Sensing. *J. Am. Chem. Soc.* **2008**, *130*, 5416−5417.
(18) Gonzalez, D. C.; Savariar, E. N.; Thayumanavan, S. Fluorescence Patterns from Supramolecular Polymer Assembly and Disassembly for Sensing Metallo- and Nonmetalloproteins. *J. Am. Chem. Soc.* **2009**, *131*, 7708−7716.
(19) Azagarsamy, M. A.; Yesilyurt, V.; Thayumanavan, S. Disassembly of Dendritic Micellar Containers Due to Protein Binding. *J. Am. Chem. Soc.* **2010**, *132*, 4550−4551.
(20) Jia, L.; Xu, L.; Wang, Z.; Xu, J.; Ji, J. Label-Free Fluorescent Sensor for Probing Heparin-Protein Interaction Based on Supramolecular Assemblies. *Chin. J. Chem.* **2014**, *32*, 85−90.
(21) Chakraborty, T.; Chakraborty, I.; Moulik, S. P.; Ghosh, S. Physicochemical Studies on Pepsin-Ctab Interaction: Energetics and Structural Changes. *J. Phys. Chem. B* **2007**, *111*, 2736−2746.
(22) Miller, R.; Fainerman, V. B.; Makievski, A. V.; Kragel, J.; Grigoriev, D. O.; Kazakov, V. N.; Sinyachenko, O. V. Dynamics of Protein and Mixed Protein/Surfactant Adsorption Layers at the Water/Fluid Interface. *Adv. Colloid Interface Sci.* **2000**, *86*, 39−82.
(23) Ezzell, S. A.; McCormik, C. L. *Water-Soluble Polymers: Synthesis, Solution Properties and Applications;* ACS Symposium Series 467; American Chemical Society: Washington, DC, 1991.
(24) Ding, L.; Liu, Y.; Cao, Y.; Wang, L.; Xin, Y.; Fang, Y. A Single Fluorescent Self-Assembled Monolayer Film Sensor with Discriminatory Power. *J. Mater. Chem.* **2012**, *22*, 11574−11582.
(25) Ding, L.; Bai, Y.; Cao, Y.; Ren, G.; Blanchard, G. J.; Fang, Y. Micelle-Induced Versatile Sensing Behavior of Bispyrene-Based Fluorescent Molecular Sensor for Picric Acid and Pyx Explosives. *Langmuir* **2014**, *30*, 7645−7653.
(26) Arnostova, H.; Kucerova, Z.; Tislerova, I.; Trnka, T.; Ticha, M. Affinity Chromatography of Porcine Pepsin on Different Types of Immobilized 3,5-Diiodo-L-Tyrosine. *J. Chromatogr., A* **2001**, *911*, 211−216.
(27) Kučerová, Z.; Majercaková, P. Immobilized-Metal-Ion Affinity Chromatography as a Tool for the Qualitative Study of Pepsinogen Phosphorylation. *J. Biochem. Biophys. Methods* **2001**, *49*, 523−531.
(28) Novotná, L.; Hrubý, M.; Beneš, M. J.; Kučerová, Z. Affinity Chromatography of Porcine Pepsin a Using Quinolin-8-Ol as Ligand. *J. Chromatogr., A* **2005**, *1084*, 108−112.
(29) Tatemichi, M.; Sakamoto, M.-a.; Mizuhata, M.; Deki, S.; Takeuchi, T. Protein-Templated Organic/Inorganic Hybrid Materials Prepared by Liquid-Phase Deposition. *J. Am. Chem. Soc.* **2007**, *129*, 10906−10910.
(30) Pluhar, B.; Ziener, U.; Mizaikoff, B. Surface Imprinting of Pepsin Via Miniemulsion Polymerization. *J. Mater. Chem. B* **2013**, *1*, 5489−5495.
(31) Eissa, S.; L'Hocine, L.; Siaj, M.; Zourob, M. A Graphene-Based Label-Free Voltammetric Immunosensor for Sensitive Detection of the Egg Allergen Ovalbumin. *Analyst* **2013**, *138*, 4378−4384.
(32) Note: In the absence of DTAB, the fluroescence variation upon addition of pepsin and o-egg for a period of 30 min is more due to the unstablity of the fluroescence of the probe in water (cf. Figure S1, Supporting Information).
(33) Ianeselli, L.; Zhang, F.; Skoda, M. W.; Jacobs, R. M.; Martin, R. A.; Callow, S.; Prevost, S.; Schreiber, F. Protein-Protein Interactions in Ovalbumin Solutions Studied by Small-Angle Scattering: Effect of Ionic Strength and the Chemical Nature of Cations. *J. Phys. Chem. B* **2010**, *114*, 3776−3783.
(34) Liu, B.; Wang, J.; Zhang, G.; Bai, R.; Pang, Y. Flavone-Based Esipt Ratiometric Chemodosimeter for Detection of Cysteine in Living Cells. *ACS Appl. Mater. Interfaces* **2014**, *6*, 4402−4407.

DOI: 10.1021/am508421n
ACS Appl. Mater. Interfaces 2015, 7, 4728−4736